

## **General Disclaimer**

### **One or more of the Following Statements may affect this Document**

- This document has been reproduced from the best copy furnished by the organizational source. It is being released in the interest of making available as much information as possible.
- This document may contain data, which exceeds the sheet parameters. It was furnished in this condition by the organizational source and is the best copy available.
- This document may contain tone-on-tone or color graphs, charts and/or pictures, which have been reproduced in black and white.
- This document is paginated as submitted by the original source.
- Portions of this document are not fully legible due to the historical nature of some of the material. However, it is the best reproduction available from the original submission.



## Technical Memorandum 79554

# Lateral Density Anomalies and the Earth's Gravitational Field

B. E. Lowrey

MAY 1978

National Aeronautics and  
Space Administration

**Goddard Space Flight Center**  
Greenbelt, Maryland 20771

(NASA-TM-79554) LATERAL DENSITY ANOMALIES  
AND THE EARTH'S GRAVITATIONAL FIELD (NASA)  
51 p HC A04/MF A01 CSCL 08N

N78-30754

Unclas  
29335

G3/46

LATERAL DENSITY ANOMALIES AND THE EARTH'S  
GRAVITATIONAL FIELD

B. E. Lowrey

Measurement Evaluations Branch, Code 932

ABSTRACT

The interpretation of gravity is valuable for understanding lithospheric plate motion and mantle convection. This paper compares postulated models of anomalous mass distributions in the earth with the observed geopotential as expressed in the spherical harmonic expansion. In particular, models of the anomalous density as a function of radius are found which can closely match the average magnitude of the spherical harmonic coefficients of a degree  $\ell$ . These models include (1) a two-component model consisting of an anomalous layer at  $\sim 200$  km depth (below the earth's surface) and at  $\sim 1500$  km depth (2) a two-component model where the upper component is distributed in the region between 1000 and 2800 km depth, (3) a model with density anomalies which continuously increase with depth more than an order of magnitude. Models of anomalous density spread into laterally extended caps or confined to depths above 1000 km do not match the properties of the observed field unless very special and unlikely arrangements of anomalous densities are assumed. If the average coefficient in a degree of the geopotential is a consequence of anomalous densities which vary as a function of radius, then only models in which the anomalous densities increase with depth and extend to great depth, probably to the core-mantle boundary, appear able to match the geopotential. The most reasonable geophysical interpretation of deep lateral density variations is that they are associated with lower mantle convection.

CONTENTS

	<u>Page</u>
ABSTRACT .....	iii
I. INTRODUCTION .....	1
Procedure .....	3
II. RESULTS OF SIMULATION OF STOKES COEFFICIENTS	
FROM DENSITY MODELS .....	7
a. Mass Point as a Function of Depth .....	7
b. Mass Point as a Function of Geographic Location .....	13
c. Column and Random Layer Distributions .....	16
d. Extended Sources .....	24
III. INTERPRETATION .....	29
IV. CONCLUSIONS .....	38
ACKNOWLEDGMENTS .....	40
REFERENCES .....	41

## ILLUSTRATIONS

<u>Figure</u>	<u>Page</u>
1 Relative Amplitude of the GEM-9 Field Model . . . . .	8
2 Relative Amplitude of the SAO II Field Model . . . . .	9
3 Effect of Depth on the Relative Amplitude. . . . .	10
4 Relative Amplitude of a Mass Point at 1,000 and 1,500 km Depth ( $m = 1.7 \times 10^{-5}$ em). . . . .	12
5 Third Degree Legendre Polynomials vs. Latitude . . . . .	15
6 Relative Amplitude from Anomalies Above 1,000 km Depth . . . . .	17
7 Relative Amplitude from an Anomalous Layer at 1,500 km Depth. . . . .	19
8 Relative Amplitude from a a Two Component Model . . . . .	20
9 Relative Amplitude from a Continuously Increasing Density Model . . . . .	22
10 Continuously Increasing Density Model—The Contribution of Each Layer to the Second Degree Amplitude. . . . .	23
11 Relative Amplitude of Layered Caps . . . . .	26
12 Relative Amplitude of a Convection Roll . . . . .	28

## TABLES

<u>Table</u>	<u>Page</u>
1 Twelfth Degree Field from a Polar Mascon. . . . .	13
2 Twelfth Degree Field from an Equatorial Mascon. . . . .	14

# LATERAL DENSITY ANOMALIES AND THE EARTH'S GRAVITATIONAL FIELD

## I. INTRODUCTION

An unresolved problem of geophysics is the motive force of plate tectonics. Since the motion of plates is strongly correlated with earthquakes, information which may help to understand this motion is useful. While it is generally agreed that plate motion is associated with convective motion, the question of whether this convection is confined to the upper mantle or arises from the lower mantle is controversial at present. It is the purpose of this paper to study the relation of mass anomalies to the geopotential in order that the results may be used to support, refute or aid in developing geophysical hypotheses concerning mantle motions.

The lateral density anomalies are of significance in studying mass imbalances due to convection. The radial distribution of density contributes only to the central force term of the geopotential and is obtained from a combination of geophysical and astronomical data and Monte Carlo calculations (Haddon and Bullen, 1969; Press, 1970; Gilbert, Dziewonski and Brune, 1973). These computations provide a density  $\rho(r)$  to which anomalous densities are referred. These lateral density anomalies  $\Delta\rho$  do not alter the amount of mass in a spherically symmetric shell when summed over the shell.

Lateral density anomalies are expressed in the coefficients of the terms above the first degree and order in the spherical harmonic expansion of the geopotential. Satellite perturbation data has been used to derive an extensive set of coefficients for the spherical harmonic expansion of the geopotential. These coefficients, often termed "C's and S's" are particularly convenient to extract from long arc satellite orbits. Often, there are individual coefficients which are resonant with a particular satellite's orbit and may be individually determined

(Wagner, 1976; King-Hele, Walker and Gooding, 1974, 1975; Klokocnik, 1975). More generally, geopotential field models are constructed by simultaneously solving for the coefficients from large data bases constructed from many satellite orbits (Lerch et al., 1977; Gaposchkin, 1974). The satellite arcs include a variety of inclinations, periods and mean distances from the earth and therefore yield a data base which spans the globe. A global distribution is necessary to make a meaningful determination of the coefficients as they are computed from a global integration. The global knowledge allows the possibility of separating global contributions from local contributions and of estimating the structure of lateral density variations as a function of depth.

But although the spherical harmonic expansion contains global geophysical information, the extraction of this geophysical information is not a straightforward procedure. The major difficulty is that knowledge of the the external potential does not allow a unique mathematical inversion procedure to recover internal density variations. An additional difficulty is that the density variations within the earth probably are not distributed in the shape of any individual harmonic with the exception of the hydrostatic bulge of the earth. The hydrostatic bulge is mainly expressed in the second (zonal) harmonic, constituting the overwhelming proportion of it, and 1/4 of the fourth zonal harmonic. The hydrostatic contribution is well understood (Jeffreys, 1963), and this paper considers possible models of the nonhydrostatic part of the earth's potential using the method of calculating the nonhydrostatic spherical harmonics from assumed density distribution.

There have been several previous investigations of the geophysical implications of the spherical harmonic coefficients of the earth's gravity field. Allan (1972), using a method of analysis initially described by Cook (1967) and employed by Guier and Newton (1965), and Khan (1970), concluded that the earth's potential could be modeled in terms of two components

where the harmonics below degree 6 or 8 could be described by density anomalies at an effective depth below the earth's surface of  $\sim 1700$  km, and higher harmonics at a depth of  $\sim 300$  km. Khan (1977) and Lambeck (1976), using essentially similar techniques of analysis concluded that all harmonics could be described by anomalies distributed between 0 and 800-1000 km depth. Suggested sources of the earth's gravitational field also include the core-mantle interface (Hide and Horai, 1968; Hide and Malin, 1970; Khan and Woolard, 1970), the upper mantle transitions zones (Bott, 1971), and the upper mantle (Higbie and Stacey, 1970). Occasionally attempts have been made to interpret individual harmonic coefficients with particular features (Khan and O'Keefe, 1974); Wang, 1966). McDonald (1963) suggested that the non-hydrostatic portion of the second harmonic was a fossil bulge remaining from an earlier rate of rotation of the earth.

This paper utilizes the approach employed by Goldreich and Toomre (1969) and by Pollack (1973): a mass distribution is postulated and the resulting coefficients of the spherical harmonics are calculated. Whereas Goldreich and Toomre calculated only the effect of random mass distributions on the second harmonics, this paper calculates the harmonics up to degree and order 25. This approach investigates the mathematical implications of converting a lateral anomalous density into spherical harmonics first and then compares the results with actual field models and other geophysical data or theory. In this way, no geophysical assumptions are required initially (except that the density anomalies are small in comparison with the density) and a number of plausible geophysical configurations are investigated. These include mass points, plumes, convection rolls, extended caps and randomly distributed masspoints covering layers on the globe. The variation in anomalies with depth is studied in the two limiting cases; assuming the anomalies to be in a narrow layer—single depth—and assuming the anomalies to be distributed throughout most of the earth's mantle. An

important difference in this work is that the results of simulation are compared with observed average coefficient values in each degree, rather than basing conclusions on a least square fit which has been summed over all degrees. The ability of a model to satisfy all degrees equally provides a more stringent criterion to evaluate the model.

### Procedure

The external potential of the gravity of the earth satisfies LaPlace's Equation (MacMillan, 1958)

$$\nabla^2 V = 0 \quad (1)$$

The external potential may be expressed as

$$V = V_1 + V_2$$

where  $V_1 = GM/r$  is the potential of a central force. The anomalous external potential  $V_2$  is

$$V_2 = GM \sum_{\ell=0}^{\infty} \sum_{m=0}^{\ell} \frac{a_e^{\ell}}{r^{\ell+1}} \bar{P}_{\ell m}(\sin \phi) (\bar{C}_{\ell m} \cos m\lambda + \bar{S}_{\ell m} \sin m\lambda) \quad (2)$$

where  $G$  is the Newtonian gravitational constant,  $M$  the total mass of the earth,  $a_e$  the radius of the earth,  $\phi$  the latitude,  $\lambda$  the longitude,  $r$  the distance from the center of the earth and  $\bar{P}_{\ell m}$  are normalized spherical harmonics or associated Legendre polynomials. The  $\bar{C}_{\ell m}$  and  $\bar{S}_{\ell m}$  are estimated from data such as satellite perturbations, altimetry and ground-based data.

The normalized coefficients are more suitable for geophysical interpretation as the unnormalized coefficients are related to the normalized coefficients by a factor of  $\left[2(2\ell + 1) \frac{(\ell - m)!}{(\ell + m)!}\right]^{1/2}$  if  $m \neq 0$  and  $(2\ell + 1)^{1/2}$  if  $m = 0$  and thus the unnormalized tesserals decline rapidly in a given degree  $\ell$ . This effect in the unnormalized coefficient along with the circumstance that only the zonals are of any import in the hydrostatic field, has in the past sometimes caused the tesserals to be considered of less importance.

If a density distribution due to a set of mass points  $m_i$  is assumed, the resulting spherical harmonic coefficients can be calculated readily:

$$\begin{aligned}\bar{C}_{\ell m} &= \sum_i m_i \left( \frac{a_e - d_i}{a_e} \right)^\ell \frac{1}{(2\ell + 1)} \bar{P}_{\ell m}(\sin \phi_i) \cos m \lambda_i \\ \bar{S}_{\ell m} &= \sum_i m_i \left( \frac{a_e - d_i}{a_e} \right)^\ell \frac{1}{(2\ell + 1)} \bar{P}_{\ell m}(\sin \phi_i) \sin m \lambda_i\end{aligned}\quad (3)$$

where  $m_i$  is a "mass point," normalized to the earth's mass and located at depth  $d_i$  below the surface of the earth, latitude  $\phi_i$  and longitude  $\lambda_i$ . The point mass form is most convenient numerically but the mass may be spread in a volume element having density  $\Delta\rho_i$  in which case the above equation would take the form of an integral rather than a summation. The coefficients of the potential of a unit spherical cap on the earth's surface are

$$\begin{bmatrix} \bar{C}_{\ell m} \\ \bar{S}_{\ell m} \end{bmatrix} = \frac{\bar{P}_{\ell+1}(\cos \alpha) - P_{\ell-1}(\cos \alpha)}{(2\ell + 1)^2 (1 - \cos \alpha)} \bar{P}_{\ell m}(\sin \phi) \begin{bmatrix} \cos m \lambda \\ \sin m \lambda \end{bmatrix}\quad (4)$$

where  $\alpha$  is the generating angle of the cap (Pollack, 1973). The computation is generalized for a mass  $m$  at a depth  $d$  by the factor  $m \left( \frac{a_e - d}{a_e} \right)^\ell$ .

The amplitude of a degree is often used to make correlations with geophysical properties.

The quantity

$$\sigma_\ell^2 = \sum_{m=0}^{\ell} (\bar{C}_{\ell m}^2 + \bar{S}_{\ell m}^2)\quad (5)$$

is often termed the "degree variance" or the "power spectrum" or the "spectral energy."

This dimensionless quantity is rotationally invariant. It is related to the root mean square coefficient variation  $\langle \bar{C}_{\ell m} \text{ or } \bar{S}_{\ell m} \rangle$  in a degree  $\ell$ :

$$\sigma_\ell^2 = (2\ell + 1) \langle \bar{C}_{\ell m}^2, \bar{S}_{\ell m}^2 \rangle\quad (6)$$

Kaula (1966) observed that the harmonics follow this empirical rule:

$$\langle \overline{C}_{\ell m}, \overline{S}_{\ell m} \rangle = 10^{-5} / \ell^2 \quad (7)$$

Pollack (1973) noted that the degree variance of a unit mass point on the surface of the earth may be normalized by multiplying by  $(2\ell + 1)$ . This motivated his definition of the quantity

$$\Phi_{\ell} = \sigma_{\ell} (2\ell + 1)^{1/2} \quad (8)$$

where a mass point of unit value of the surface of the earth will have  $\Phi_{\ell}(\ell) = 1$  at all degrees. This quantity is here termed the "relative amplitude" since it reflects the amplitude of a degree computed from an arbitrary mass distribution relative to the amplitude of a degree computed for a unit surface mass point. The relative amplitude is used in this paper to study the spectral properties of the harmonics because it is convenient for geophysical interpretation and graphical presentation. As Pollack showed,  $\Phi_{\ell}$  computed for a given total mass will diminish with degree when the mass is lowered from the surface or spread into a regular extended feature. A field arising from non-organized crustal density distributions will exhibit a flat behavior of  $\Phi_{\ell}$  as  $\ell$  increases.

## II. RESULTS OF SIMULATION OF STOKES COEFFICIENTS FROM DENSITY MODELS

This section shows the results of actual numerical experiments obtained from postulating various mass distributions and calculating sets of coefficients in the spherical harmonic expansion of the geopotential (Eq. 3). The resulting coefficients or the general properties of a set of coefficients are compared with the actual coefficients measured in satellite geodesy. This is a fruitful approach because the associated Legendre polynomials in Eq. 3 are too complicated to allow an intuitive grasp of the effect of a mass configuration on the spherical harmonic coefficients and because it is possible to develop general statistical properties of a set of coefficients. It is not possible with this approach to infer a unique mass distribution but it is possible to evaluate the ability of interesting or geophysically plausible mass configurations to explain the gravitational field. The configurations used for simulations include a mass point, a vertical column of mass points, an extended spherical cap, sets of random mass points globally distributed at various depths, sets of concentric caps and convection rolls.

Modern fields are now obtained to high degree and order. The relative amplitudes ( $\Phi_q$  from Eq. 8) for two field models, GEM-9 (Lerch et al., 1977) and SAO-II (Gaposchkin and Lambeck, 1971) are shown in Fig. 1 and Fig. 2. It is noted that this quantity declines by a factor of 4 between degree 3 and degree 8 and declines less precipitously in higher degrees.

### a. Mass Point as a Function of Depth

The spherical harmonic coefficients are simulated for a disturbing field composed of one mass point. This particularly simple distribution is able to demonstrate interesting general properties. The behavior of the relative amplitude as a function of degree is shown in Fig. 3 for mass points at three depths, 0 km, 500 km and 1500 km. Pollack (1973) showed that a point mass produces the 'richest spectrum' when the relative amplitude is compared with that

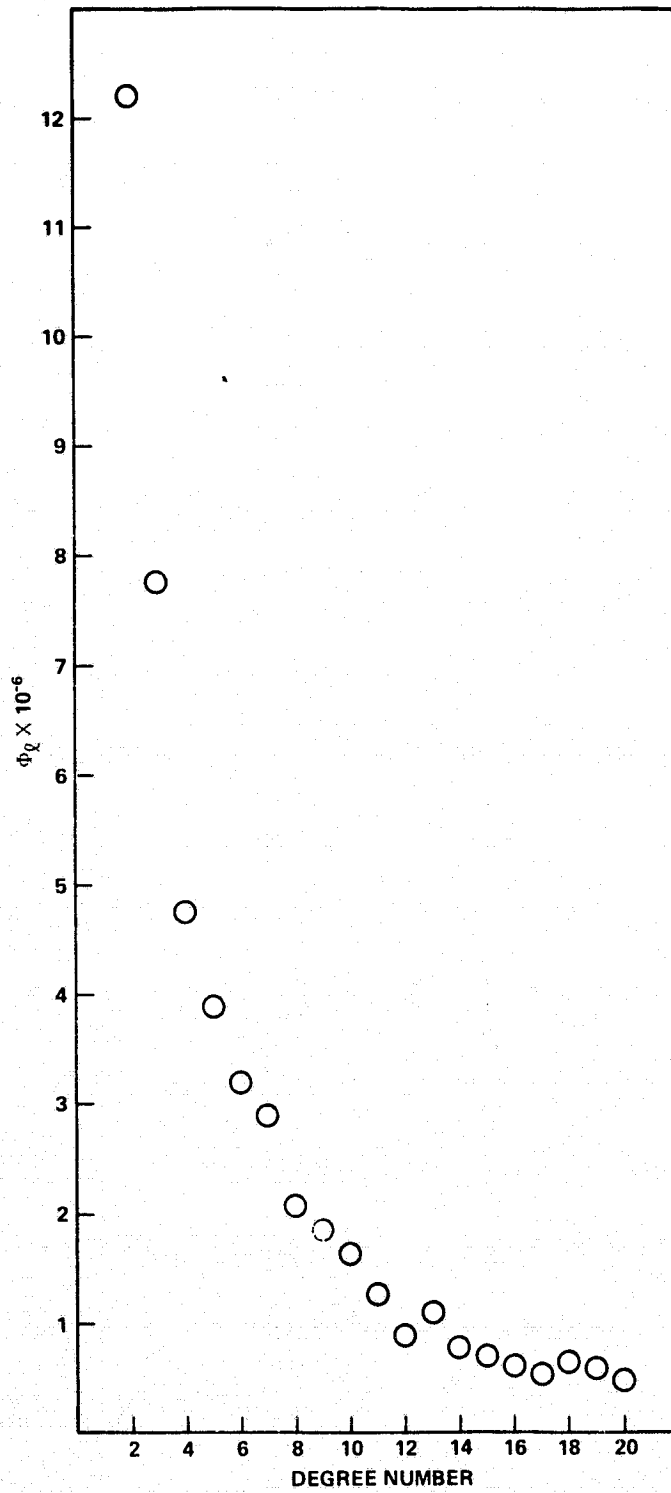


Figure 1. Relative Amplitude of the GEM-9 Field Model

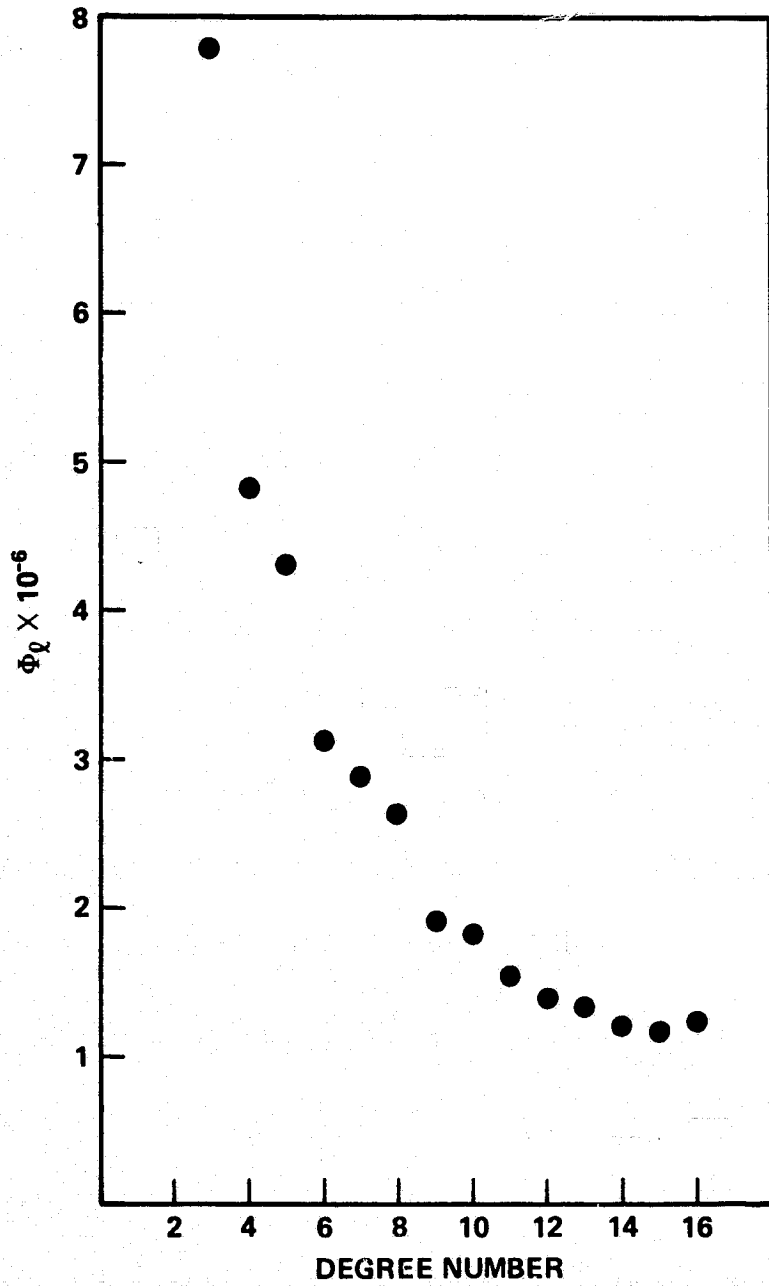


Figure 2. Relative Amplitude of the SAO II Field Model

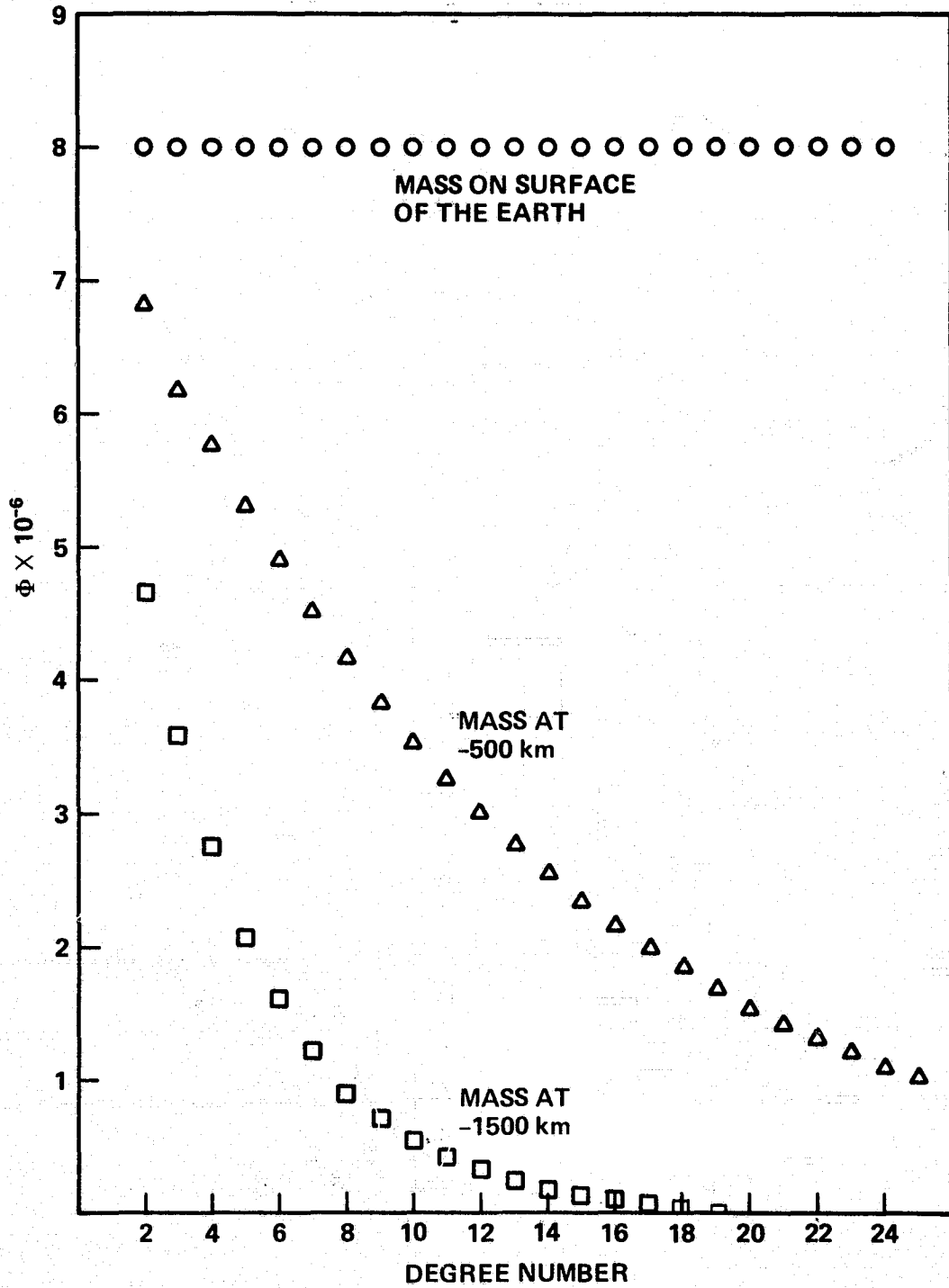


Figure 3. Effect of Depth on Relative Amplitude

arising from extended sources such as a spherical cap or a spherical rectangular block. Also, if a density anomaly is less than  $5^\circ$  in lateral extent, the decline of  $\Phi_\ell$  is not substantially different from  $\Phi_1$  to a point mass in the harmonics below degree and order 30. Therefore, although the mass point is not a completely realistic geophysical model, it is useful in describing the contribution of a short wavelength density anomaly.

If a mass point is placed on the surface of the earth, the relative amplitude is constant and equal to the value of the mass in earth mass (em) units. Thus a mass point of  $8. \times 10^{-6}$  em produces a value of  $\Phi_\ell = 8. \times 10^{-6}$  em for all  $\ell$ . If the mass point is placed slightly below the earth's surface, then  $\Phi_\ell$  will decline with increasing degree and even the contribution to degree two will be diminished. At a depth of 500 km, a mass of  $8. \times 10^{-6}$  em gives  $\Phi_2 = 7. \times 10^{-6}$ , at 1500 km  $\Phi_2 = 5. \times 10^{-6}$ . This effect increases sharply with increasing degree, according to the factor  $\left(\frac{a_c - h}{a_c}\right)^2$  in eq. 3 so that deep anomalies, as for example at the core-mantle interface, will not contribute to more than the low degree harmonics, if at all perceptible in the earth's measured field.

In comparing the decline of the relative amplitude of the low degree terms with that of a real field, the decline of the real field up to degree 12 is followed most closely by a mass point at 1500 km depth. After degree 13, the real field does not decline as steeply as a mass point at 1000 km depth. But, below degree 12, the real field cannot be matched by a point mass located above 1000 km depth. This result derived from a mass point assumption suggesting that the field arises from a source located below 1000 km depth is consistent with earlier findings by Allan (1972), who used similar assumptions. The magnitude of a mass point matched to a low degree field originating at a depth of 1500 km is  $1.7 \times 10^{-5}$  em (1 em =  $6 \times 10^{24}$  kg) located at depth = 1500 km (Fig 4). If placed at 1000 km depth, this mass does not match  $\Phi_\ell$ , except for the second harmonic.

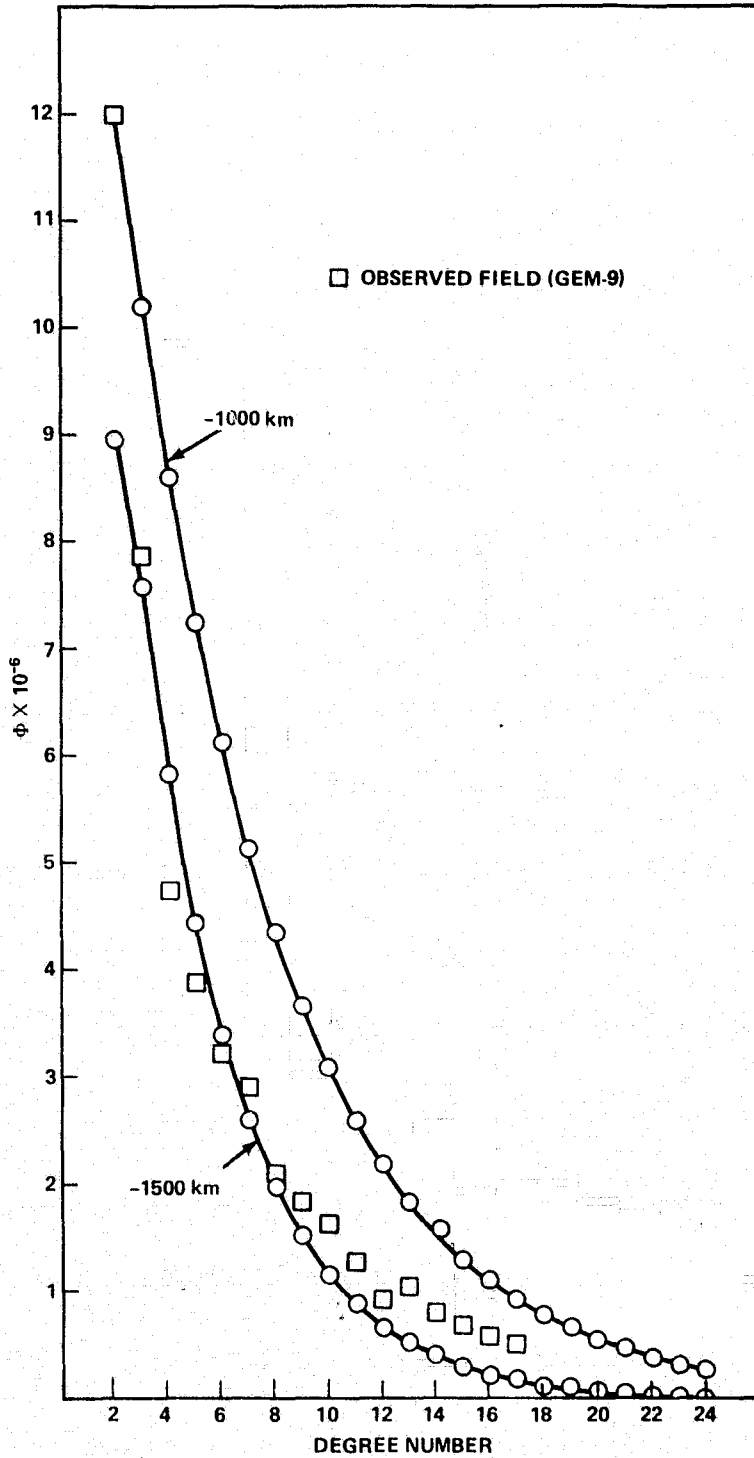


Figure 4. Relative Amplitude From a Mass Point at 1,000 and 1,500 km Depth  
 $(m = 1.7 \times 10^{-5} \text{ em})$

b. Mass Point as a Function of Geographic Location

The properties of the relative amplitude discussed above are independent of the geographic location of the mass point (by the rotational invariance of spherical harmonics); however, the geographic location of a mass point on a sphere controls the distribution of the amplitude in a degree  $\ell$  among the  $m$  orders. There is a particularly striking effect when the point mass is located near the poles or in a high latitude; the zonal and low order tesserals contain all the magnitude and the higher order tesserals and sectorial contribute negligibly to the degree. Table 1 contains a list of the  $C_{12,m}$  computed for a mass anomaly located near the pole: the magnitude of the coefficients declines strongly with increasing order. Similar effects are

Table 1  
Twelfth Degree Field from a Polar Mascon

m	$\bar{C}_{12-m}$	
1	$0.22 \times 10^{-06}$	LAT = 76° LONG = 180° HEIGHT = 0. MASS = $-\frac{1}{4} \times 10^{-6}$ em
2	$-0.34 \times 10^{-06}$	
3	$0.22 \times 10^{-06}$	
4	$-0.93 \times 10^{-07}$	
5	$0.29 \times 10^{-07}$	
6	$-0.71 \times 10^{-08}$	
7	$0.13 \times 10^{-08}$	
8	$-0.22 \times 10^{-09}$	
9	$0.28 \times 10^{-10}$	
10	$-0.29 \times 10^{-11}$	
11	$0.22 \times 10^{-12}$	
12	$-0.11 \times 10^{-13}$	

apparent at all degrees. Mass points near the equator produce no decline in the normalized coefficients of the potential field. Table 2 shows the values of  $\bar{C}_{12,m}$  for a mass point located near the equator. These equal values of the coefficients for all orders  $m$  is compatible with the behavior of the real field. The discrepancy between the behavior of a polar and equatorial mass distribution is a direct consequence of the numerical behavior of the normalized Legendre polynomials: Fig 5 show  $\bar{P}_{30}$ ,  $\bar{P}_{31}$ ,  $\bar{P}_{32}$ , and  $\bar{P}_{33}$  as a function of latitude. This decline in amplitude as a function of order as the latitude increases becomes more pronounced as the degree increases. A field arising from only density anomalies located at high latitudes would be a mainly zonal field.

Table 2  
Twelfth Degree Field from an Equatorial Mascon

m	$\bar{C}_{12-m}$	
1	$-0.14 \times 10^{-07}$	<p data-bbox="872 1178 1008 1210">LAT = 20°</p> <p data-bbox="872 1240 1048 1271">LONG = 200°</p> <p data-bbox="872 1301 1039 1333">HEIGHT = 0.</p> <p data-bbox="872 1363 1148 1395">MASS = <math>\frac{1}{4} \times 10^{-6}</math> em</p>
2	$0.49 \times 10^{-08}$	
3	$0.74 \times 10^{-08}$	
4	$-0.16 \times 10^{-08}$	
5	$0.22 \times 10^{-08}$	
6	$-0.69 \times 10^{-08}$	
7	$-0.60 \times 10^{-08}$	
8	$0.17 \times 10^{-07}$	
9	$-0.33 \times 10^{-08}$	
10	$-0.17 \times 10^{-07}$	
11	$0.18 \times 10^{-07}$	
12	$-0.67 \times 10^{-08}$	

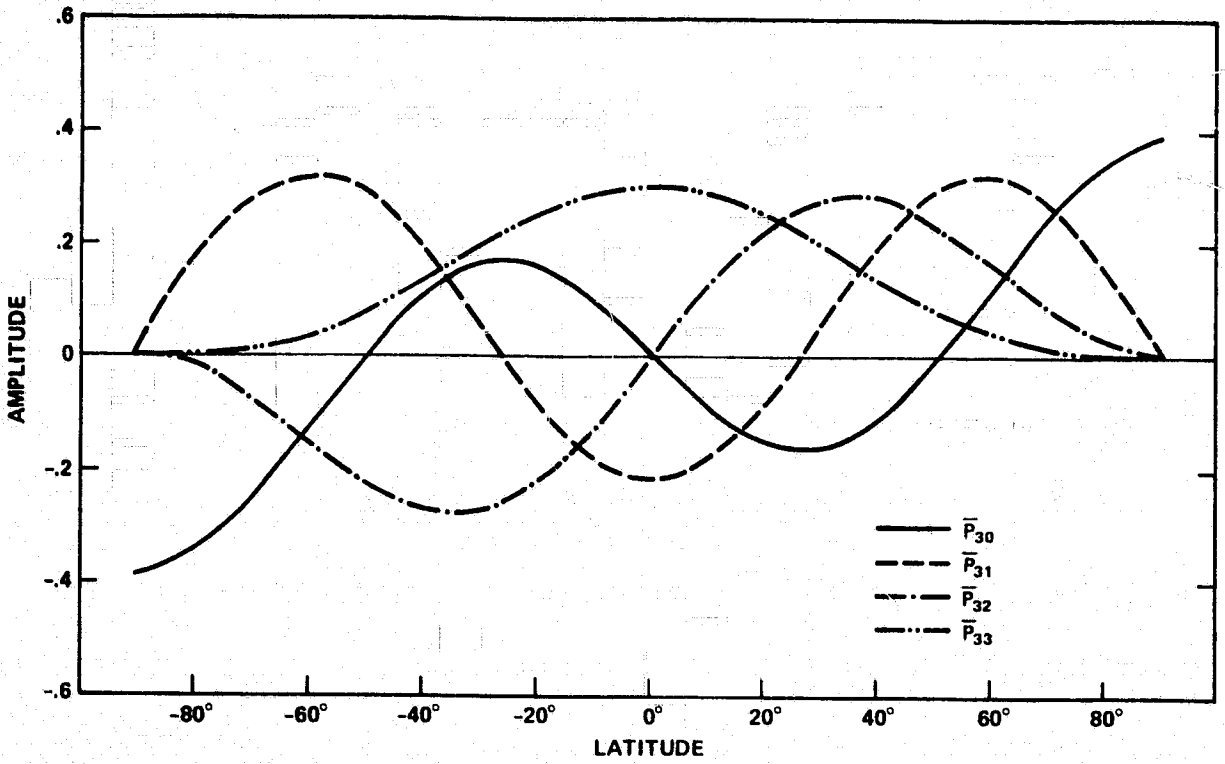


Figure 5. Third Degree Legendre Polynomials vs. Latitude

These results should be considered in discussions of the source of "the third harmonic" (Khan and O'Keefe, 1974; Kaula, 1972); it is pointed out here that an "Antarctic anomaly" invoked to explain the high value of  $\bar{C}_{30} = .95 \times 10^{-6}$  cannot simultaneously explain the high value of  $\bar{S}_{33} = 1.4 \times 10^{-6}$ . In fact, numerical explorations failed to locate any point on the globe which could satisfactorily represent all the third harmonics, including the largest, the  $\bar{C}_{31} = 2.0 \times 10^{-6}$ .

### c. Column and Random Layer Distributions

The effect of distributions extending through a range of depths was investigated using a local distribution arranged in a column of point masses and a global distribution consisting of mass points with random magnitudes inserted into equal area blocks. The local anomaly was studied using a column of masses at the same geographic location placed at depths of 100 km apart. The global distribution was investigated by constructing layers separated by 100 km in depth composed of random valued mass points placed in equal area blocks.

The simplest construction of reflecting anomalies at many depths is a column of equal-valued mass points. A column of 11 mass points, located at the same geographic position (latitude =  $20^\circ$ , longitude =  $200^\circ$ ) but varying in depth location by 100 km, was constructed placing a mass point of  $.5 \times 10^{-6}$  em at 0 km, -100 km, -200 . . -1000 km. The relative amplitude resulting from this configuration is the smooth line shown in Fig. 6.

Similar results were obtained from a set of 11 global layers placed at 0, -100, -200, . . . . -1000 km. Each infinitesimally thin layer was constructed by dividing the spherical surface into equal-area  $10^\circ \times 10^\circ$  blocks (Paul, 1973) and inserting a random mass point into each block. The random value of the mass point was generated from a Gaussian distribution taken about 0 with a standard deviation of  $2 \times 10^{-8}$  earth masses. The results are shown as squares in Fig. 6. These results are compatible with those from the column of mass points,

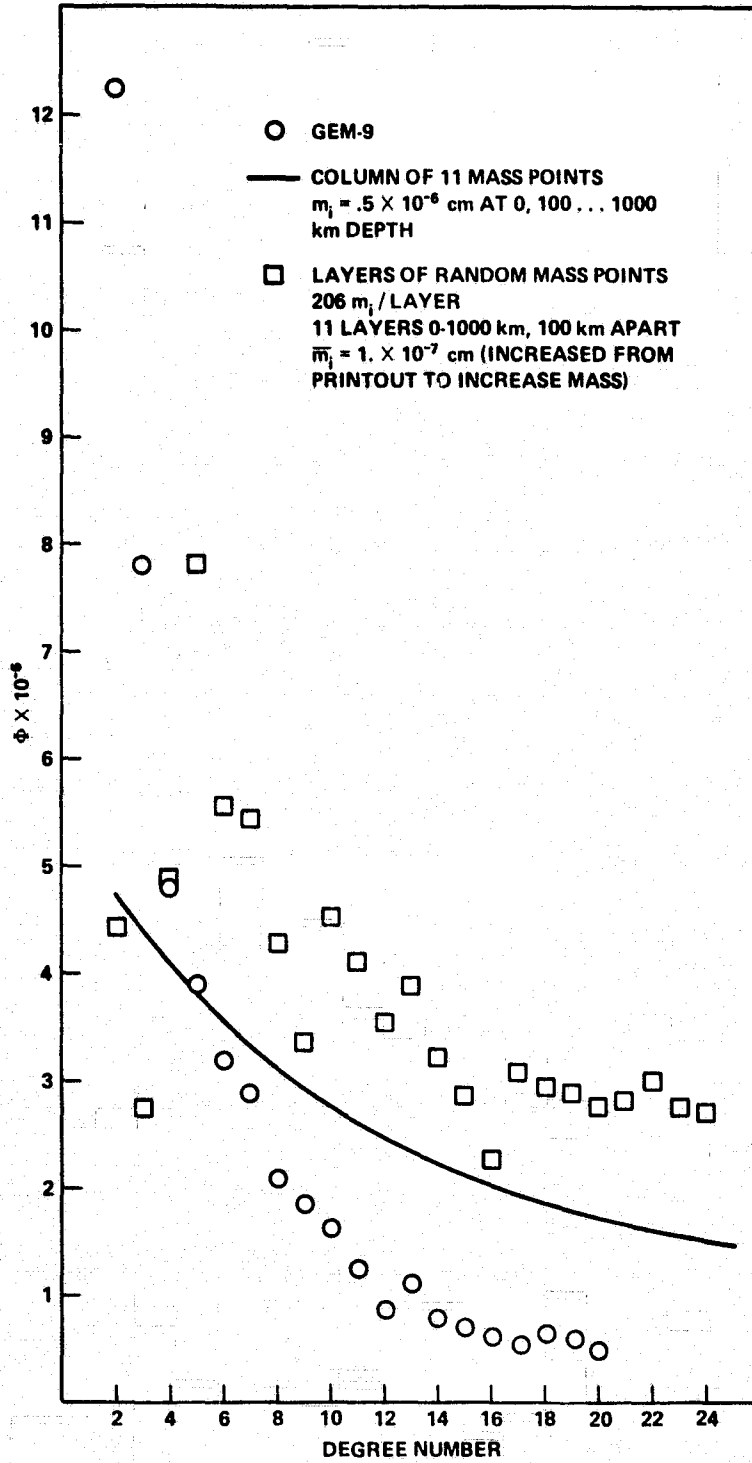


Figure 6. Relative Amplitude from Anomalies Above 1,000 km Depth

except for a slight offset of the curve due to a slightly different effective mass. The global layer of mass points, which is in essence modeling short wavelength uncorrelated anomalies, produces relative amplitude that scatters about the smooth line resulting from an individual column. In comparing with a field model, indicated in Fig. 6 by circles, the simulated energy spectra cannot reproduce the sharp decline in the low degrees. Even if the harmonics below four are deleted, the simulated amplitudes do not decline as rapidly as the observed. Further, it was found that random layers of equal anomalous densities which begin at the surface and extend to depths down to the core-mantle interface do not produce substantially different fields from those extending to only 1000 km. Thus an anomalous field of uncorrelated short wavelength features with equal mass per spherical area at each depth would not usually produce the observed field.

A single global layer of random mass points at a depth of 1500 km does replicate the decline of the relative amplitude of the real field in the low orders as shown in Fig. 7. The layer was constructed by placing 206 mass points averaging  $1 \times 10^{-6}$  em in  $10^\circ \times 10^\circ$  global equal area blocks. The overall decline of the  $\Phi$  is well-matched but these differences remain 1) the random field produces more scattered values of the low degree harmonics 2) the observed high degree harmonics ( $l > 12$ ) do not vanish as do the modeled, a difference corrected by adding an upper component similar to the 'two-component' model obtained by Allan (1972).

The assumption of two narrow layers of density anomalies imposed severe geophysical constraints, and so a modification of the two-component model was investigated, where the low degree component was spread in layers between 1000 and 2800 km depth. Fig. 8 shows the relative amplitude of a two-component model assuming masses of  $1. \times 10^{-6}$  em arranged in a column of 19 points at 1000, 1100, 1200 . . . 2800 km depth and one mass point at

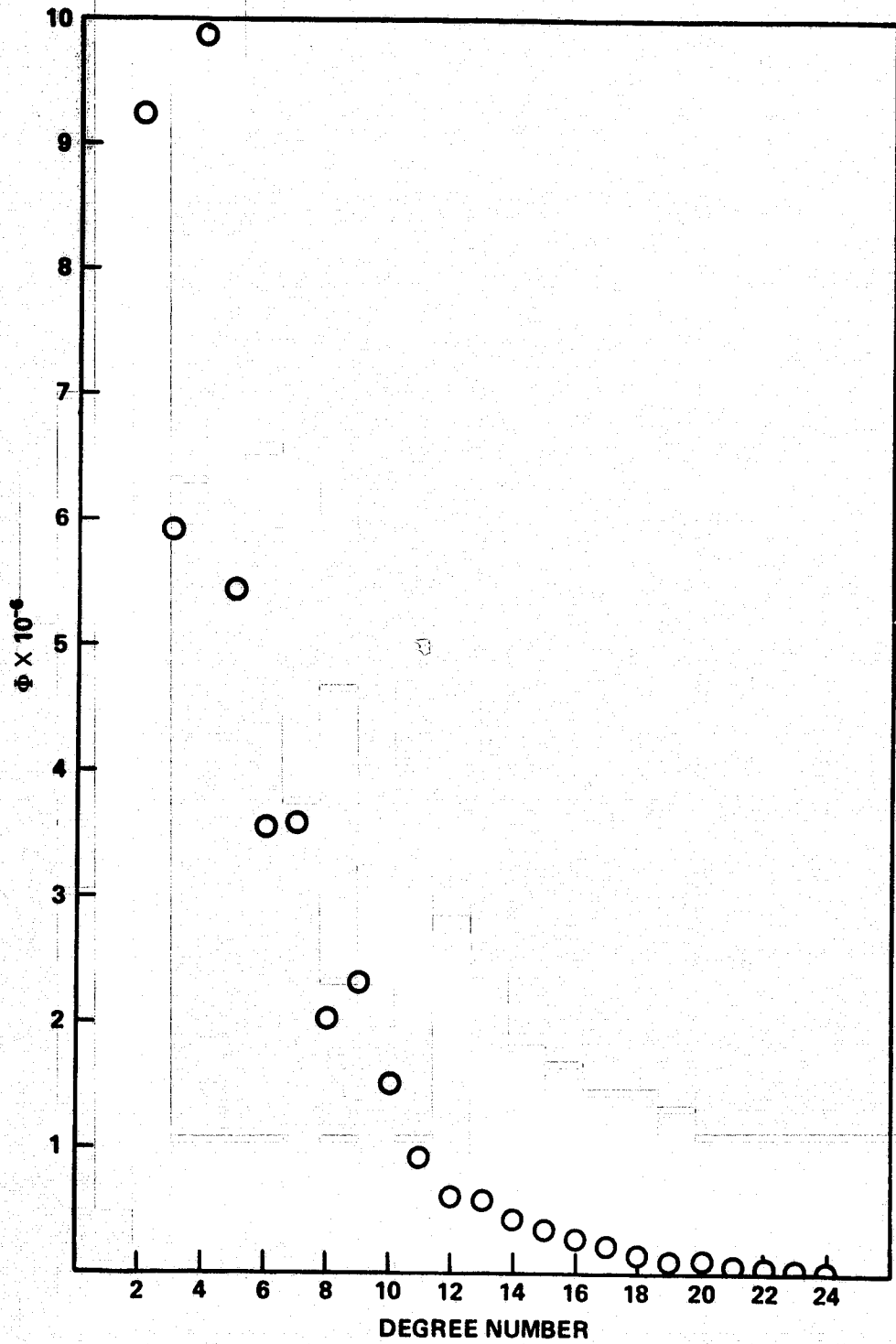


Figure 7. Relative Amplitude from an Anomalous Layer at 1,500 km Depth

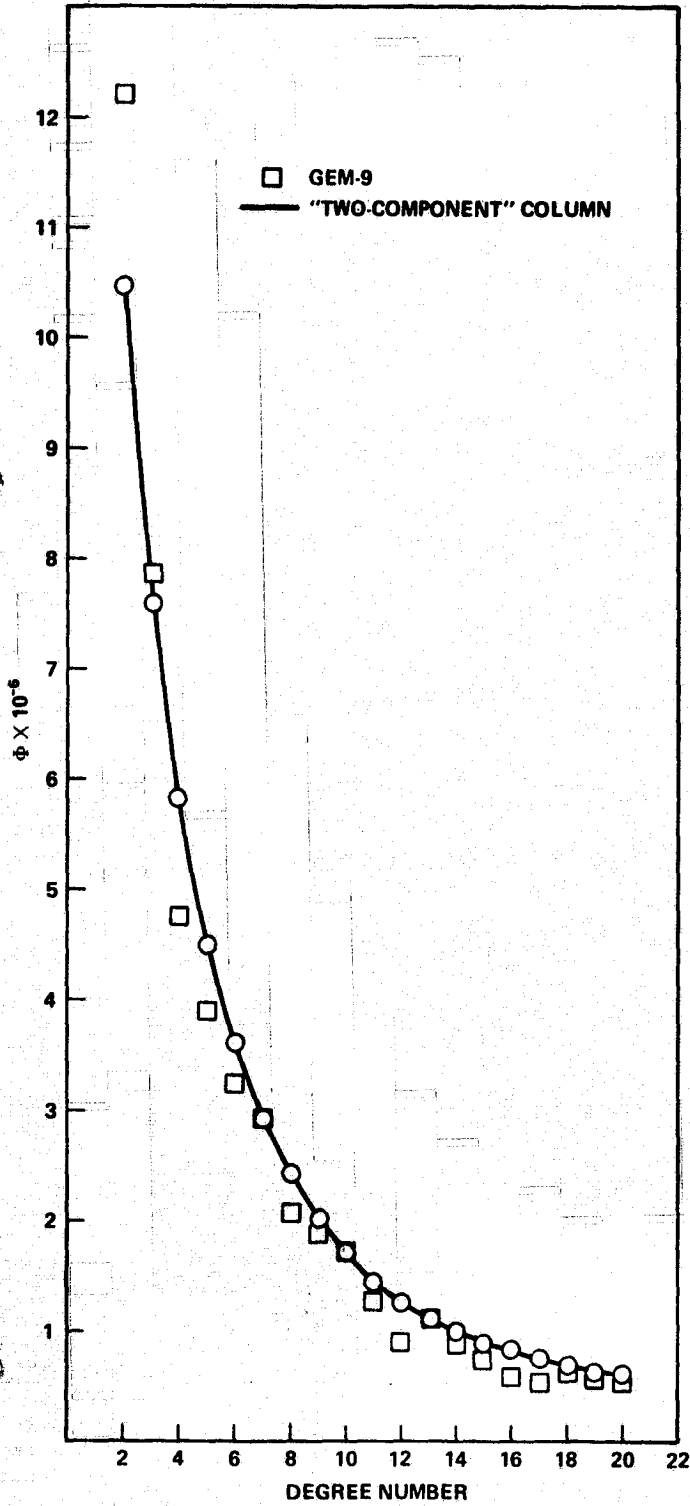


Figure 8. Relative Amplitude from a Two Component Model

200 km depth. (The high degree component could just as well be modeled by spreading the density anomaly at 200 km depth through several hundred km because the relative amplitude does not resolve between these two possibilities.) The  $\Phi$  of this modified two-component model matches that of the observed field well. This model implies a greatly increased anomalous density for the lower component because the deep mass points are placed every 100 km apart whereas there is only one mass point in the upper 1000 km.

Because the modified two-component model places possibly artificial constraints on the density variations, a model employing monotonically increasing density anomalies was tested. In this model, an effective mass of  $.25 \times 10^{-6}$  em was placed on the surface layer and a mass incremented by  $.025 \times 10^{-6}$  em was placed on each successive layer deeper by 100 km, that is,  $m_i = .250 \times 10^{-6}$  at 0 km,  $.275 \times 10^{-6}$  at 100 km,  $.300 \times 10^{-6}$  at 200 km,  $.325 \times 10^{-6}$  at 300 km, . . . .  $.95 \times 10^{-6}$  at 2800 km depth. This produced relative amplitudes (Fig. 9) with properties similar to that observed, and a reasonable match in magnitudes. Very close matches in magnitude can be obtained by any one of a number of possible adjustments in density variation. Also, discontinuities in anomalous density such as are known to occur in the radial distribution of density can reproduce the observed energy spectrum since the spherical harmonic coefficients do not resolve this type of model differences. The mass points vary by a factor of 4 from the surface to the core-mantle interface. Considering that the area of a layer shrinks by a factor of 4 in this distance, this model implies that the anomalous density increases by a factor of 16 at the bottom of the mantle.

In order to investigate the origins of the second harmonic, the percentage contribution to the  $\Phi_2$  (amplitude of the second degree harmonic) from each depth can be computed (Fig. 10). Each of the 29 layers contributes between 2.5 and 3.5% of the total value of  $\Phi_2$ ; resulting in a nearly flat curve with a broad maximum between 1000 and 2000 km depth.

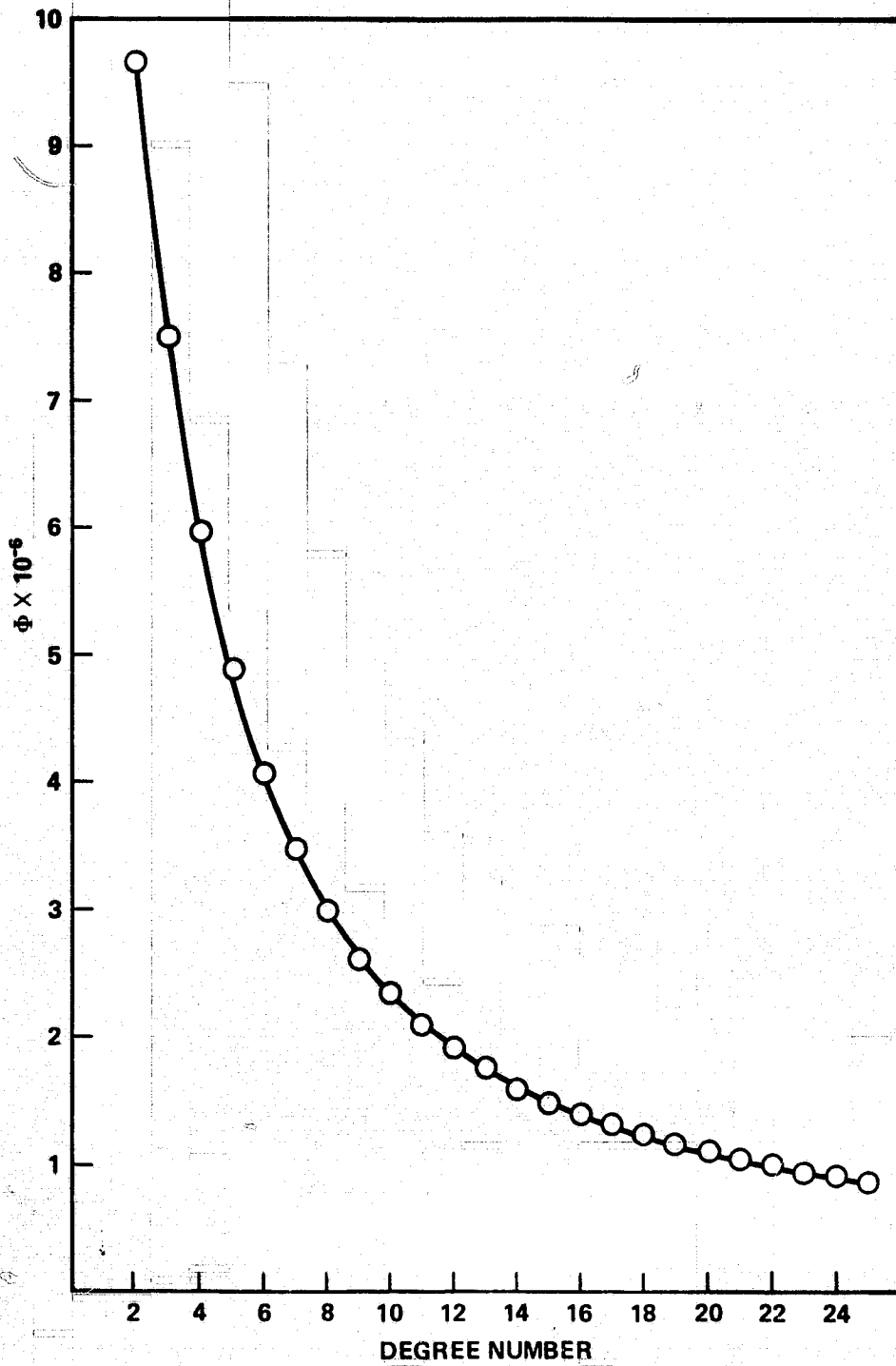


Figure 9. Relative Amplitude from a Continuously Increasing Density Model

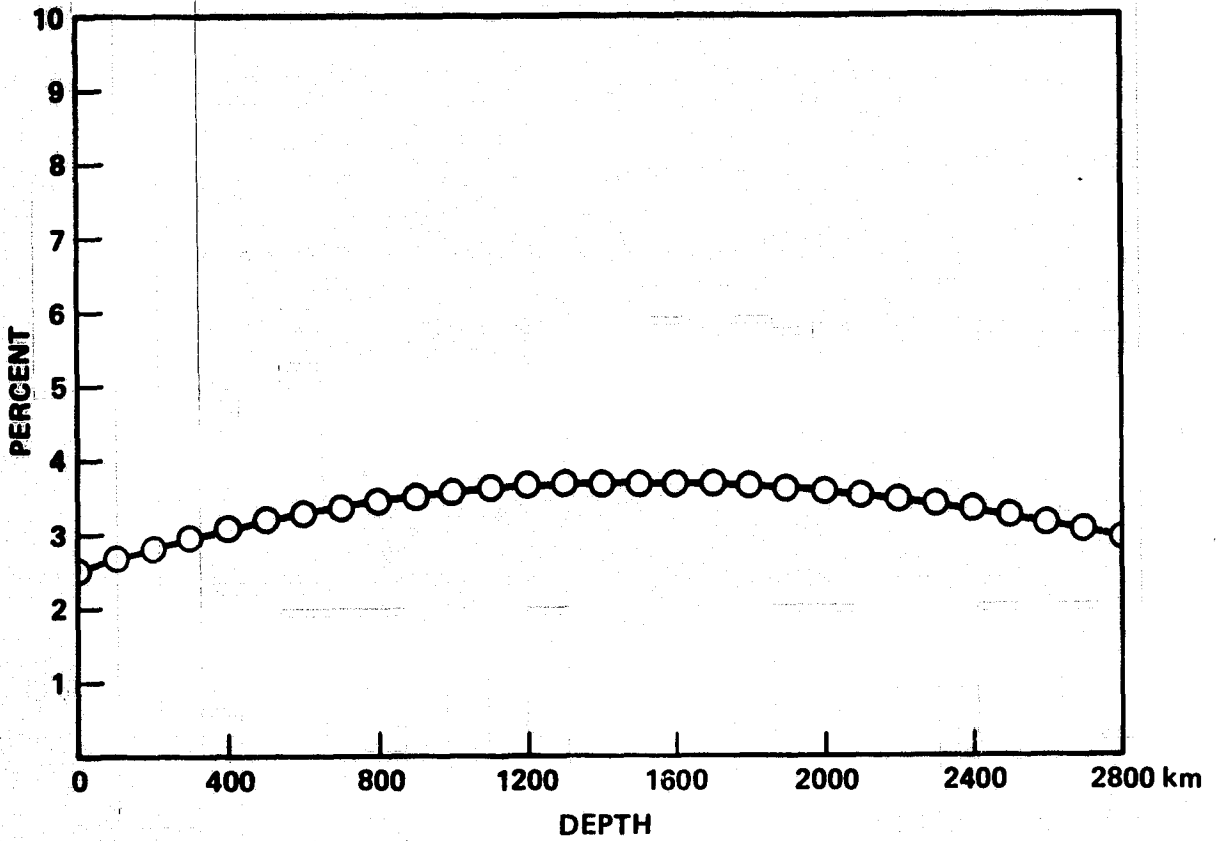


Figure 10. Continuously Increasing Density Model—The Contribution of Each Layer to the Second Degree Amplitude

2000 km depth. This monotonically increasing density model provides no single layer or region which can be said to produce the second harmonics.

The scatter produced by the field composed of individual mass points is a function of the number of anomalies involved. Investigations with a set of 827 mass points inside  $5^\circ \times 5^\circ$  equal area blocks and 92 mass points inside  $15^\circ \times 15^\circ$  blocks produced results in accord with those expected from considering the problem as a random walk process. The scatter is highest in the low degrees as a statistical consequence of summing over fewer values of  $\bar{C}_{\rho m}$  and  $\bar{S}_{\rho m}$ . As the number  $N$  of mass points increases, the net values of  $\Phi_\rho$  tend to increase as  $\sqrt{N}$ . A set of  $N$  masses of  $m_i$  each on a layer yield an effective mass equal to the total mass divided by  $\sqrt{N}$ , that is,  $m_{\text{eff}} = \frac{Nm_i}{\sqrt{N}} = \sqrt{Nm_i}$ . Vertical inhomogenities combine in the same manner, except that the strength of a layer is diminished according to the depth.

#### Extended Sources

The relative amplitude  $\Phi_\rho$  is not only a function of the depth of an anomalous density, it is also a function of geographic extension of the anomaly. Pollack (1973) showed the relative amplitude of a degree resulting from spherical caps or rectangles on the surface of the earth declines rapidly with degree if the anomalous source covers a significant area on the surface. The slope of the decline increases as the area of the lateral extension increases. The impact of a cap on  $\Phi_\rho$  is computed, where a cap is defined as a circular area on a shell generated by a central angle  $\alpha$ . For a cap of radius  $\alpha = 5^\circ$ ,  $\Phi_\rho$  is nearly like a point mass; after  $\ell = 20$ ,  $\Phi_\rho$  was reduced to about 70% of that of an equivalent mass point. However,  $\Phi_\rho$  from a  $10^\circ$  cap was reduced over an order of magnitude by  $\ell = 20$ . As the radius of the cap increases, the decline of  $\Phi_\rho$  is no longer monotonic; a strong cycloidal behavior occurs, although the oscillations are still superimposed on a declining trend. The amplitude of a  $30^\circ$  cap has declined

an order of magnitude by  $\ell = 7$ , and of a  $60^\circ$  cap by degree 3. Pollack also found that mass anomalies in the shape of a rectangle on a spherical shell produced similar results for  $\Phi_q$ .

The computations in this study confirmed Pollack's results and considered spherical caps with more structure than uniform density. By constructing a set of spherical caps with a common center but with varying radii, a layered density can be simulated. These layered cap with mass anomalies increasing toward the center are used to model features observed in the real gravity field.

Two models of layered caps were constructed for the Antarctic low using the geoidal anomalies shown in Khan and O'Keefe (1974). One cap was modelled after the anomaly referred to the reference ellipsoid (flattening  $f = 1/298.255$ ) and one cap to an ellipsoid with hydrostatic flattening ( $f = 1/299.75$ ). The model anomalous to the reference ellipsoid is centered at  $\phi = 72^\circ\text{S}$ ,  $\lambda = 183^\circ\text{E}$ . It is composed of a set of superposed concentric caps having  $m_i = -1.3 \times 10^{-6}$  em in a  $20^\circ$  cap,  $-.6 \times 10^{-6}$  em in a  $14^\circ$  cap,  $-.83 \times 10^{-6}$  em in a  $10^\circ$  cap,  $-.2 \times 10^{-6}$  in a  $7^\circ$  cap and  $-.1 \times 10^{-6}$  em in a  $4^\circ$  cap. The model referred to the ellipsoid with a hydrostatic flattening is centered at  $\phi = 76^\circ\text{S}$ ,  $\lambda = 177^\circ\text{E}$ , and consists of caps of size  $26^\circ$  with  $-1.3 \times 10^{-6}$  em,  $18.2^\circ$  with  $-.6 \times 10^{-6}$  em,  $11.3^\circ$  with  $-.3 \times 10^{-6}$  em,  $8.8^\circ$  with  $-.2 \times 10^{-6}$  em and  $6.2^\circ$  with  $-.1 \times 10^{-6}$  em. All caps were assumed to be on the surface of the earth. The  $\Phi_q$  calculated for both models dropped an order of magnitude in the first 20 degrees (Fig. 11). The two models produced similar curves, except that the hydrostatic flattening model varied slightly faster and showed the beginnings of a cycloidal shape in the first 25 degrees. An extended feature located at a depth would show a steeper decline in the relative amplitude. If an extended feature contains an intense central anomaly relative to the fringes, the relative amplitude will tend toward that of a mass point.

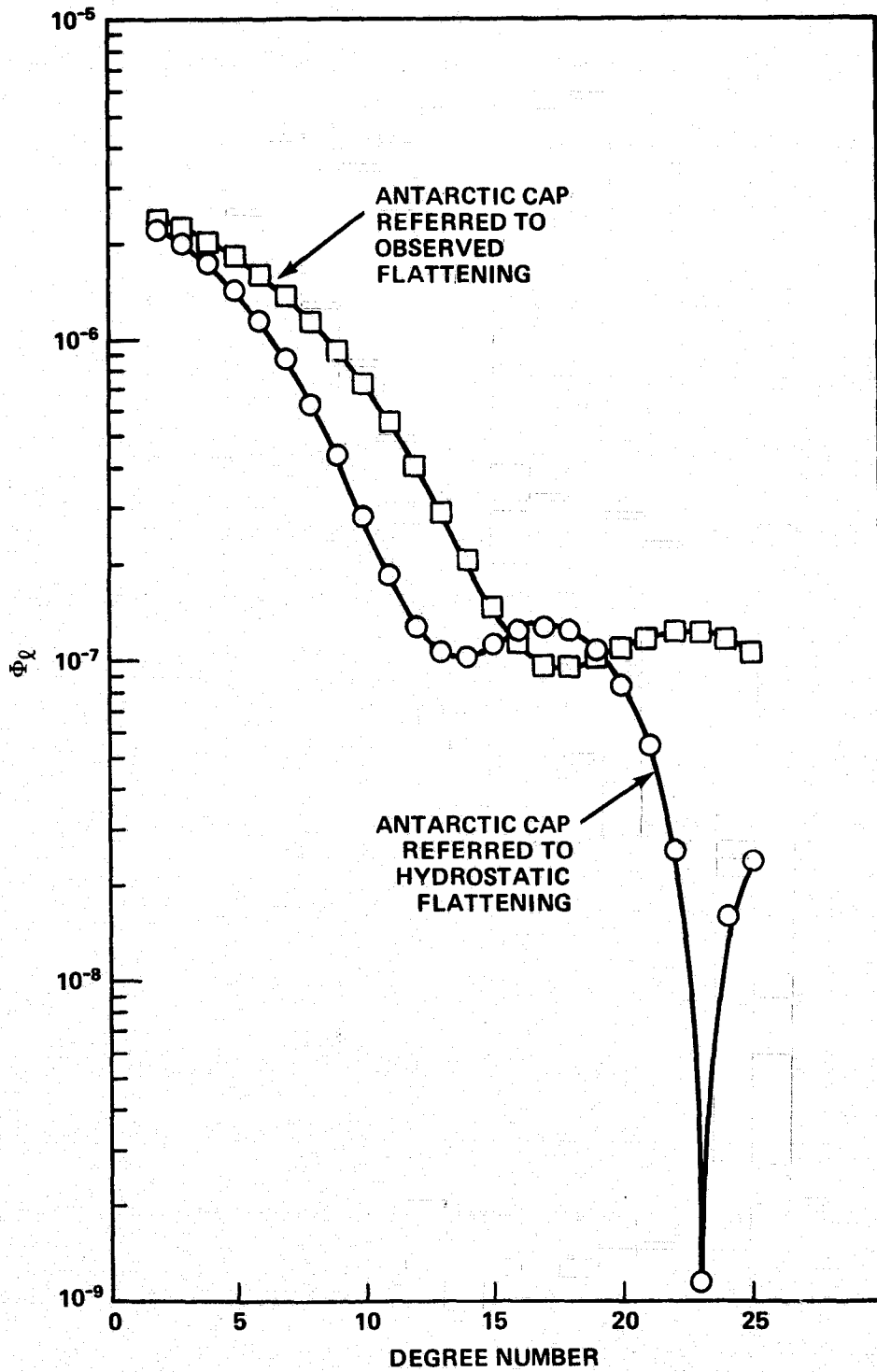


Figure 11. Relative Amplitude of Layered Caps

Thus, regular extended features near the earth's surface demonstrate a sharp decrease in  $\Phi$  with degree. Further, this decrease differs from that of the real field and of fields simulated from depth in that the decline is convex rather than concave. Therefore, this type of feature does not readily match the observed field; further, short wavelength anomalies can be expected to predominate as the degree of the field increases.

Organized surface elements may have unpredictable amplitudes. Convection rolls provided a motivation for simulations of an organized type of extended source. The possibility of convection rolls underneath the Pacific plate was calculated from theoretical considerations by Richter and Parsons (1975) and tentatively identified in the observed field above degree 12 by Marsh and Marsh (1976). This type of anomaly was modeled with 4 longitudinal rows separated by  $6^\circ$  of longitude and spanning  $9^\circ$  of latitude. Each row consisted of 10 mass points of magnitude  $\pm 1 \times 10^{-6}$  em each. Alternate rows on the earth's surface from  $\phi = 20$  to  $29^\circ$  contain positive mass points at  $\lambda = 150^\circ$ , negative masses at  $\lambda = 156^\circ$ , positive at  $\lambda = 162^\circ$  and negative at  $\lambda = 168^\circ$ . The relative amplitude of this organized element is markedly different from random or extended features. The resulting  $\Phi_q$  shown in Fig. 12 increases non-monotonically with high degree. The expected average  $\Phi_q$  from a set of 40 random mass points of  $1 \times 10^{-6}$  em on the surface is  $\sim 6. \times 10^{-6}$  for all degrees. The  $\Phi_q$  for the modeled convection roll is  $14. \times 10^{-6}$  at degree 25, over twice that of an equivalent set of random mass points. Thus organized elements in the earth's crust may contribute significantly to high degrees in a definitely non-intuitive manner.

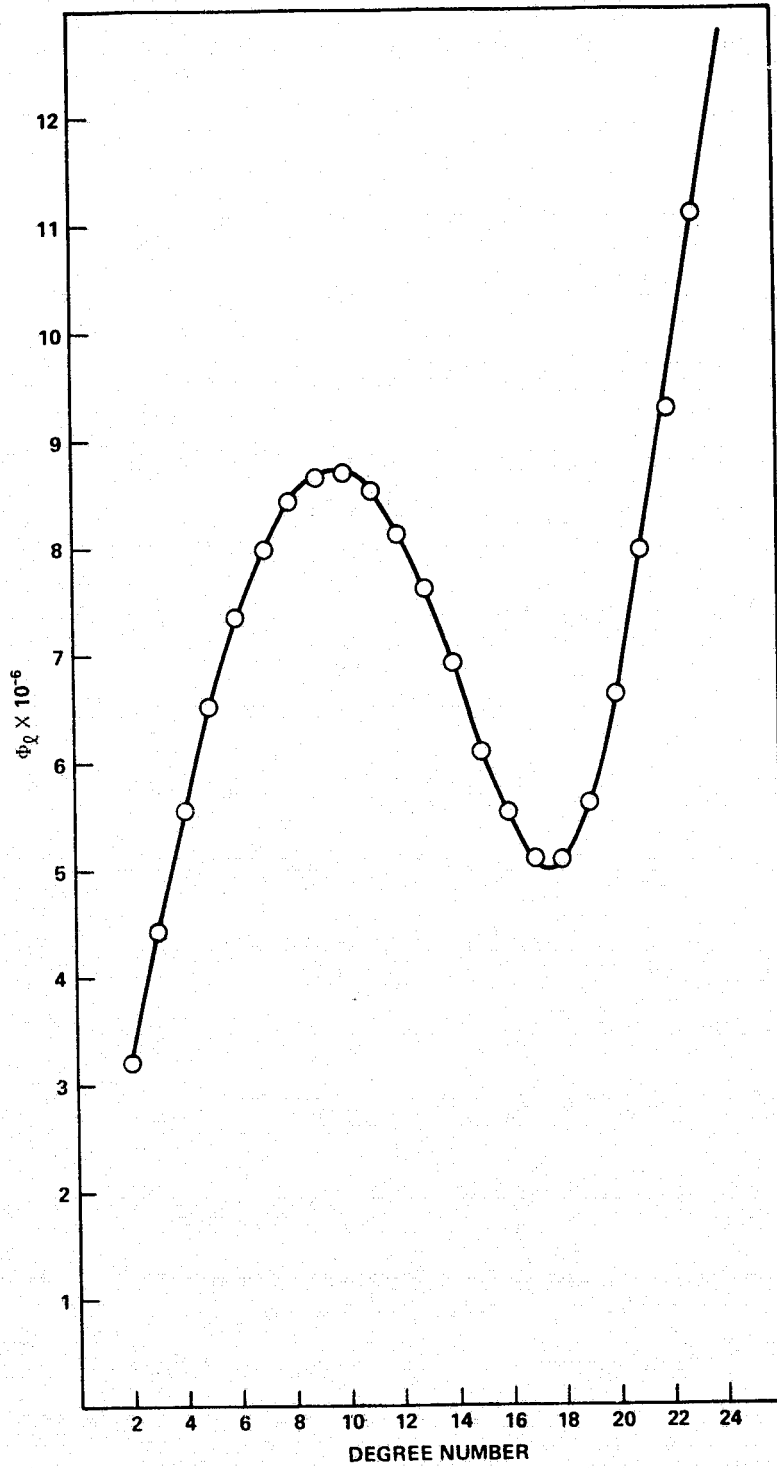


Figure 12. Relative Amplitude of a Convection Roll

### III. INTERPRETATION

The origin of the non-hydrostatic second zonal harmonic has been a source of speculation since the artificial satellite data determined a value of  $C_{20}$  in excess of that predicted by hydrostatic theory. MacDonald (1963) postulated that  $\Delta C_{20}$ , the observed excess over the hydrostatic flattening due to the rotation of the earth, was a 'fossil' bulge remanent from the earth's faster rotation rate 10 m yr ago. Maintenance of the fossil bulge required a deeper mantle viscosity of  $10^{26}$  poises, too high to allow mantle convection. Goldreich and Toomre (1969) showed that the ratio of the normalized non-hydrostatic  $\Delta \bar{C}_{20} / \bar{C}_{22}$  amounted to only 2.4 rather than the non-normalized ratio of 12 obtained by MacDonald and that this remaining excess can be explained as an artifact of the coordinate system. Wang (1966) suggested that the non-hydrostatic  $\Delta \bar{C}_{20}$  resulted from Pleistocene glaciation; O'Connell (1971) showed that the non-hydrostatic bulge is 3 times too large to be accounted for by deglaciation; also, the results obtained above indicate that a field arising from excess polar anomalies will produce a high ratio of  $\Delta C_{20} / C_{22}$ . A glacial origin of the third harmonic has also been discussed: Khan and O'Keefe (1974) compare the large negative Antarctic anomaly with the shrinkage of the ice cap in the Pliocene, although there is the difficulty of explaining the slow recovery from the melting of the ice load 4-5 m yr ago. This paper finds two additional difficulties: the mass deficiency of  $2.3 \times 10^{22}$  g postulated in the above paper does not account more than for 1/3 of the observed zonal harmonic, and this suggestion cannot begin to explain the largest third harmonic coefficients: the GEM-9 field gives  $\bar{C}_{31} = 2.02 \times 10^{-6}$  and  $\bar{S}_{33} = 1.41 \times 10^{-6}$ , whereas the  $\bar{C}_{30} = .95 \times 10^{-6}$  (Lerch, F. J. et al., 1977).

Hide and Horai (1968) suggested the second harmonic could be attributed to undulations of the core-mantle boundary, but that the stresses required to support the undulations increased dramatically with the order of the harmonics taken. Seismic wave reflections from the

core-mantle interface have demonstrated that boundary undulations of more than 5-10 km do not exist (Engdahl and Johnson, 1974; Buchbinder, 1968).

Higbie and Stacey (1970) sought a single depth where all harmonic orders would produce comparable stresses. Their results were field-dependent, but they conclude that anomalies from depths below 900 km could not explain the fields.

A widely employed method has considered the density anomalies as short wavelength features which are uncorrelated beyond brief distances. This method was outlined by Cook (1967) and employed by Guier and Newton (1965), Allan (1972), Khan (1977) and Lambeck (1976). Conclusions obtained from this technique were not always consistent: Allan favored a two-component field with effective depths of anomalous regions at 1700 km and 250 km with a larger anomalous density at the lower layer, while Khan (1977) and Lambeck (1976) concluded that the measured anomalies arise from regions above 800-1000 km. The mass point technique employed in this paper is theoretically equivalent to this technique and is used to evaluate the above conclusions.

In the simulations described in the section above, it was found that considerable variations occur naturally in the low degree harmonics with changes of density models, changes either of type or of geographic position. Further, large sets of globally distributed random anomalies produce widely varying values of the second and third harmonics. Simulations of one mass point failed to locate a point on the globe which could simultaneously supply the larger third harmonic coefficients. Therefore it seems that these harmonics contain insufficient information to establish any particular origin or site and that approach was abandoned in favor of analyses including all the harmonics and allowing the possibility that the density variations may be widely distributed. Implicit assumptions are that the density variations should have a reasonable magnitude and that radial distributions satisfying Kaula's 'rule of

thumb' would be sought rather than special cases of geographic positions. For example, a model confining density anomalies to a thin surface layer (in the manner of the surface density representation) is possible but unlikely since a random set of surface anomalies would not produce Kaula's 'rule of thumb'

The models considered in this paper fall into two broad classes 1) extended sources, that is long wavelength anomalies and 2) mass points, that is short wavelength anomalies. None of the models considered gravity anomalies originating from the core (below 3000 km) as it is difficult to suppose that a liquid outer core can support anomalies of any substance.

The impact of extended sources on the relative amplitude was calculated by Pollack (1973) using an even density cap. Kaula (1977) computed the 'degree variation' ( $\sigma_q$ ) using a Monte Carlo simulation of extended sources and determined that sources correlated within  $20^\circ$  best fit the observed field. He found that density anomalies must extend to 3000 km depth and that the values of decay length indicated that the anomalies must increase with depth. His model using the horizontal spacing  $\gamma_c \simeq 20^\circ$  best fit the exponent  $n$  of Kaula's rule of thumb  $10^{-5}/\varrho^n$  but the closeness of the fit to the model significantly exceeded the observed fit. In particular, the mid-degree (6-11) spectra were substantially higher than predicted by Kaula's rule of thumb. This can be understood by considering the convex curvature of the relative amplitude produced by extended sources, as shown by Pollack and demonstrated above, in contrast with the concavity of the relative amplitude of the observed field. Kaula also noted the excess scatter of the simulated models compared to the observed field.

The results above indicate that extended sources are represented more heavily in the 2nd and 3rd harmonics (in comparison with mass points). Because the variation of the second and third harmonics from any model is large, it is difficult to assess the extent of the contribution of extended sources to these coefficients. However, these harmonics seem to have

larger values than would usually occur from models of random mass points so it is possible that extended sources contribute 1/3 or 1/4 of the magnitude of these coefficients.

The abrupt decline in the relative amplitude of an extended source implies that such a feature will disappear when the long wavelengths are removed. Wagner (personal communication) has pointed out the Indian Ocean deficit is mainly represented in the low degree field ( $\ell \leq 4$ ). Gravity fields derived from local data types, rather than spherical harmonic representations may better measure extended sources. This possibility should be further studied as it is of interest in considering future techniques for gravity field recovery. Kaula (1963) noted that the observed field seemed to consist of incoherent short wavelength features; the above results demonstrate that the spherical harmonic representation of the gravity field measures such features in preference to extended features of equal mass.

Simulations did not confirm that the field may be constructed of random short wavelength anomalies of equal density extending no deeper than 1000 km. This result is not in accord with earlier findings of Lambeck (1976) and Khan (1977) and thus further consideration of this discrepancy is warranted. Lambeck estimated that the density anomalies which contribute to the measured harmonics are located at less than 800 km depth, with the power in the harmonics above degree 6 attributed to heterogeneities below 300 or 400 km. In deriving this result, he made two assumptions concerning the density variations: 1) that the power spectrum of the anomalies is the same for all layers of the spherical shells and 2) that the power spectrum may be represented by a white noise distribution. The first assumption is neither supported nor conclusively refuted by geophysical evidence. However, since there are sharp changes in density as a function of radius, it is quite possible that the average amplitude of density anomalies may also vary with the radius. Thus the first assumption imposes a serious constraint on the postulated mass distributions.

The second assumption, that the power spectrum of the density may be represented by a white noise spectrum, can be examined in greater detail. Lambeck expresses the anomalous density in spherical harmonics

$$\Delta\rho = \sum_{\ell=0}^{\infty} \sum_{m=0}^{\ell} (C_{\ell m}(\rho)P_{\ell m}(\theta) \cos m\lambda + S_{\ell m}(\rho)P_{\ell m}(\theta) \sin m\lambda)$$

and considers the power spectrum

$$V_{\ell}^2(\Delta\rho) = \sum_{m=0}^{\ell} (C_{\ell m}^2(\rho) + S_{\ell m}^2(\rho))$$

where  $V_{\ell}^2(\Delta\rho)$  is assumed to be a constant at all wavelengths. This assumed power may be compared with the spectral power of postulated density anomalies. The power of a mass point is proportional to  $1/(2\ell + 1)^{1/2}$ , as discussed above. The spectrum of the point mass is a limiting case for non-organized elements: as Pollack (1973) stated, "a point mass displays the richest harmonic spectrum at all harmonic degrees." That is, when the spectrum of a point mass is compared with extended mass distributions such as a spherical cap or spherical rectangle, that of the point mass declines less sharply with increasing degree. Further, the assumption of white noise implies that the amplitude of the shorter wavelengths are just as large as that of longer wavelengths, a geophysically unreasonable assumption. Although it is possible to construct a mass distribution approximating the power spectrum of a white noise spectrum, this is clearly a special event and may require unreasonable mass distributions. If applied to a real power spectrum, the white noise assumption will exhibit a preference for a shallow depth of origin compared to a geophysically reasonable density distribution.

Application of this technique by Khan involved the minimizing of the residuals from a function derived by Cook (1967) so that a fit to the slope could be obtained. This procedure reduces the sensitivity of the degree variance so that the result is less significant. It may be noted that all fields which are cumulative from the surface to an arbitrary depth  $D$  produce spherical harmonic coefficients which have the same order of magnitude as predicted by Kaula's rule of thumb. The differences between fields become more discernible when the relative amplitude  $\Phi_2$  employed by Pollack (1973) is used. Further, applications of Cook's technique usually involve the use of assumptions which predicate the answer in a complex manner.

The results in this paper indicate that it is unlikely that the low harmonics arise from random mass anomalies near the surface because the amplitude does not decay as steeply as that of the observed field. Further, it seems difficult to match the observed amplitude with that arising from extended sources as these produce an amplitude which as a convex slope rather than concave. Thus, the observed gravitational field is not readily explained by assuming only shallow sources.

Two models of anomalous density as a function of radius were found which did match the general characteristics of the observed relative amplitudes of the geopotential. One model is a modification of the 'two-component' model of Allan (1972), where two magnitudes of density anomalies in the upper and lower mantle are employed; the other model has density anomalies which continuously increase from the surface to the core-mantle boundary. These models represent extremes of a continuum of possible models which cannot be resolved in the external geopotential. Both models postulate deep mantle anomalies of larger magnitude than the upper mantle and crustal anomalies. Since no models without this property were found to be capable of providing a satisfactory match to the observed relative amplitude,

it is concluded that deep mantle anomalies of average magnitude larger than those of the crust and upper mantle are a geophysical property of the earth.

The modified two component model represents the lower mantle component, which forms the low degree harmonics, with layers containing an effective mass of  $1 \times 10^{-6}$  em each 100 km from 1000 km to 2800 km depth (in contrast to a single layer at 1500 km in the Allan model). The upper component, which forms the high degree harmonics, is represented by a single layer of effective mass of  $1 \times 10^{-6}$  em at 200 km depth. The lower component is larger by an order of magnitude since the upper component is the only mass in the upper 1000 km whereas the lower component has mass layers every 100 km and by an additional factor of 4 to compensate for decrease in spherical area of a layer at 3000 km depth. Thus if the upper component is distributed throughout the 1000 km, this model requires an increase in anomalous density of a factor of 40 between the surface and the core; or, if the upper component is regarded as confined to the first 200 km, this model requires a region in which the anomalous density apparently vanishes.

If the lower component is composed of 800 blocks of  $5 \times 5^\circ$  in extent and 100 km in thickness, the effective mass of  $1 \times 10^{-6}$  em at 1000 km depth may be converted to an average anomalous density  $\langle \Delta\rho \rangle = .01\text{g/cm}^3$ , and at 2800 km  $\langle \Delta\rho \rangle = .04\text{g/cm}^3$ . If, as this model may suggest, there is a region where little anomalous density exists, the geophysical implication would be that the driving force of plate tectonics would be confined to motion in the upper mantle or crust.

The modified two-component model has the additional deficiency of limiting the major contributions to the low harmonics to layers a few hundred km thick thus reducing the number  $N$  of density anomalies. Large  $N$  decreases the deviations of  $\Phi_q$  from the general

trend, which is desirable since the observed field demonstrates relatively little scatter in the  $\Phi_g$ .

The continuously increasing anomalous density model is represented by mass points spaced 100 km apart from the earth's surface to the base of the mantle and increasing linearly from  $.25 \times 10^{-6}$  gm at the surface to  $.95 \times 10^{-6}$  gm at 2800 km depth. At the surface, the average anomalous density  $\langle \Delta\rho \rangle$  in a  $5 \times 5^\circ$  block of 100 km thickness is found to be  $.0025\text{g/cm}^3$  and at 2800 km  $\langle \Delta\rho \rangle = .03\text{g/cm}^3$ . Thus a ratio of less than 1% in  $\langle \Delta\rho \rangle / \rho$  can explain the gravitational field.

This model also has the property that all layers contribute an equal amount to the second harmonic and nearly equal amounts to other low harmonics. Since the coefficients averaged over the largest number N of anomalies produce relative amplitudes with minimum scatter, this model will produce the smoothest field.

The continuously increasing anomalous density model allows that sources of geophysical energy deep within the mantle (McKenzie, 1974) can be transmitted to the crust, providing an interior origin for plate tectonics (Davies, 1977).

There is geophysical evidence for anomalous densities, including deep mantle anomalies. Seismological evidence for significant lateral variations in the lowest few hundred km of the mantle have been found by Julian and Sengupta (1973), and Jordan and Lynn (1974). Recently, a global inversion of travel times of first arrivals of compressional waves has been obtained by Dziewonski et al. (1977). The earth was divided into 5 spherical layers of depths from 0-670 km, 670-1100 km, 1100-1500 km, and 2200-2800 km. Each layer was divided into 30 blocks with dimensions of  $60^\circ$  longitude and  $36^\circ$  latitude. The data base consisted of 700,000 travel time residuals formed by differencing the observed travel time

with the travel time computed from tables such as the Jeffrey-Bullen travel time tables. An inversion procedure was used to recover the anomalous velocity within each block from the travel time residual. Two discretization patterns for blocks were used to obtain two solutions for the seismic velocity deviations within a block; the two solutions for the three lower layers were similar although the two layers above 1100 km showed little correlation between the solutions. These solutions were converted in spherical harmonic expressions for the seismic velocity deviations taken through degree and order 3. The coefficients of the seismic velocity deviation of the spherical harmonic expression were found to be correlated significantly with the ten largest significant coefficients of the geopotential. In fact, the authors found that the gravity and seismic fields could be matched exactly within the limits of the accuracy of the seismic velocity deviation data. Contour maps derived from the spherical harmonic model of the velocity anomalies indicate sizable features exist in all layers of the mantle with the largest deviations at the base of the mantle.

Maximum seismic deviations in a  $60^\circ$  block in the deepest region amount to 60 m/s. If the ratio  $\Delta v/\Delta\rho = -6(\text{km/s})/(\text{g/cm}^3)$  derived from comparing seismic and gravity field coefficients by Dziewonski et al. is employed, then  $\Delta\rho = .01$  g. This is consistent with the above values of  $\Delta\rho$ , derived from consideration of gravity alone.

The existence of deep-seated lateral seismic inhomogeneities provides independent support for deep density anomalies, in addition to the compelling evidence obtained from the simulations above.

#### IV. CONCLUSIONS

Two models of radial distribution of anomalous density were found that can replicate the energy spectrum of the observed gravitational field. Both models contained deep anomalous densities of larger magnitude than shallow anomalies. These deep anomalies extend to the base of the mantle in both models. No model of anomalous density as a function of radius can replicate the properties of the observed field as a function of degree if the density anomalies exist only above 1000 km depth. Therefore it is probable that deep and large density anomalies form a significant portion of the earth's geopotential contained in the low degree and order spherical harmonic coefficients. The minimum depth at which there must be large anomalies is 1500 km, but very large anomalies would be required unless the anomalies are extended deeper. Anomalies extending to the base of the mantle with average anomalous densities of  $\langle \Delta\rho \rangle \sim .03\text{g/cm}^3$  can represent the relative amplitude as a function of degree. Lateral variations in seismic travel times support the concept of a heterogeneous lower mantle. This concept is also in accord with the notable lack of correlation of low degree harmonics with surface features (Kaula, 1967).

The external geopotential expressed in spherical harmonics preferentially measures uncorrelated short wavelength features over long wavelength features, with the exception of the very low degrees where laterally extended features may be significant. The summation of several short wavelength features produces a noticeable scatter of the energy spectrum about the trend line produced by one similar feature. Several thousand short wavelength features may be necessary to produce a simulated field with a degree of scatter in the energy spectrum comparable to the relatively small scatter observed.

The observed value of the energy of the second harmonic is compatible in magnitude with the models, although there is an excess of  $\sim 10\%$  compared to most of the models which

well match the degrees above two. This possible excess can be attributed either to scatter, which is largest in the second degree, or to the contributions of extended features. It is not possible to recover any significant geophysical information from the non-hydrostatic second zonal harmonic, *per se*.

The two models of radial anomalous density able to represent the decline of the energy spectrum are extremes of a continuum of satisfactory models. The monotonically increasing anomalous density model postulates a continuously increasing density, where the effective anomalous mass/spherical layer has increased by a factor of 4 from the surface to the base of the mantle to about  $1 \times 10^{-6}$  earth masses at 2800 km depth. The modified two-component model postulates an effective mass of  $1 \times 10^{-6}$  em in the region between 0 and 1000 km depth and an effective mass of  $1 \times 10^{-6}$  em on spherical layers placed every 100 km between 1000 and 2800 km depth. Discontinuous changes in anomalous density where the radial density is also discontinuous are reasonable, but if so, such changes cannot be resolved in the gravity observations.

The monotonically increasing anomalous density model may be related to recent discussions of the geophysics of the mantle. In a review, O'Connell (1977) showed that the data indicates there is no compelling reason for mantle convection to be confined to the upper mantle and there is evidence that mantle convection extends to the lower mantle. Recent studies have found a uniform viscosity for the mantle (Dicke, 1969; O'Connell, 1971; Cathles, 1975). A review of thermal convection calculations together with other evidence concludes that unless there are large viscosity differences ( $\sim 10^4$ ) the flow induced by plate tectonic motion will penetrate into the lower mantle (Davies, 1977). Since the results above demonstrate that the earth's gravity field is best explained by the existence of strong deep

mantle density anomalies, it seems reasonable to suppose that lower mantle convection is the agent of plate tectonic motion rather than the consequence.

The anomalies in the crust and upper mantle predominate in the higher degree field. With the advent of high degree and order gravity fields, it became possible to correlate surface features with gravity anomalies. Kaula (1969, 1972) found strong associations of anomalies with extensive Quaternary volcanism and orogeny, active ocean rise and ocean basins. Other correlations with near surface features include long-wavelength elevations associated with cooling plates spreading from ocean rises (Sclater et al., 1975) and Pacific ocean anomalies associated with asthenospheric convection rolls (Marsh and Marsh, 1976; Richter and Parsons, 1975). These features predominate in the higher degrees; however, as Rapp (1977) showed, the degree at which an extended feature is energetic is not related in a simple manner to the angular size of the feature.

In the monotonically increasing model, every 100 km thick shell between the surface and the core of the earth provides a contribution of  $\sim 3\%$  to the energy of the non-hydrostatic second degree harmonic. In this event, the origins of the harmonic coefficients are everywhere and gravitational data must be combined with other geophysical data in order to interpret lateral density heterogeneities.

#### ACKNOWLEDGMENTS

It is a pleasure to acknowledge stimulating discussions with Paul Lowman. F. T. Heuring provided skillful computational assistance and valuable discussions. John Foreman performed very useful programming.

## REFERENCES

Allan, R. R., "Depth of sources of gravity anomalies", *Nature*, 236, p. 22-23, 1972.

Bott, M. H. P., "The mantle transition zone as possible source of global gravity anomalies", *Earth Planet. Sci. Lett.*, 11, 28-34, 1971.

Buchbinder, G. G. R., "Properties of the core-mantle boundary and observations of PcP," *J. Geophys. Res.*, 73, 5901-5923, 1968.

Cathles, L. M. III, "The viscosity of the earth's mantle"., Princeton University Press, New Jersey, 1975.

Cook, A. H., "Gravitational considerations", in *The Earth's Mantle*, edited by T. F. Gaskell, pp. 63-68, Academic, New-York, 1967.

Dicke, R. J., "Average acceleration of the earth's rotation and the viscosity of the deep mantle", *J. Geophys. Res.*, 74, 5895-5902, 1969.

Dziewonski, A. M., Hager, B. H. and R. J. O'Connell, "Large-Scale heterogeneities in the lower mantle", *J. Geophys. Res.*, 82, p. 239-255, 1977.

Engdahl, E. R. and L. E. Johnson, "Differential PcP travel times and the radius of the core", *Geophys. J. R. Astr. Soc.*, 39, 435-456, 1974.

Gaposchkin, E. M., and Lambeck, K., "Earth's gravity field to the sixteenth degree and station coordinates from satellite and terrestrial data", *J. Geophys. Res.*, 76, p. 4855-4883, 1971.

Gaposchkin, E. M., "Earth's gravity field to the eighteenth degree and geocentric coordinates for 104 stations from satellite and terrestrial data", *J. Geophys. Res.*, 79, 5377-5411, 1974.

Gilbert, F., Dziewonski, A. and Brune, J. "An informative solution to a seismological inverse problem", Proc. Nat. Acad. Sci., 70, 1410-1413, 1973.

Goldreich, P., and A. Toomre, "Some remarks on polar wandering", J. Geophys. Res., 74, p. 2555-2567, 1969.

Guier, W. H., and R. R. Newton, "The earth's gravity field as deduced from the Doppler tracking of five satellites", J. Geophys. Res., 70, 4613-4626, 1965.

Haddon, R. A. W. and Bullen, K. E., "An earth model incorporating free earth oscillation data", Phys. Earth Planet. Int., 2, 35-49, 1969.

Hide, R., and K. Horai, "On the topography of the core-mantle interface", Phys. Earth Planet. Interiors, 1, 305-308, 1968.

Hide, R. and Malin, S. R. C., "Novel correlations between global features of the earth's gravitational and magnetic fields", Nature, 225, 605-609, 1970.

Higbie, J. and Stacey, F. D., "Depth of density variations responsible for features of the satellite geoid", Phys. Earth Planet. Interiors, 4, 145-148, 1970.

Jeffreys, H., "On the hydrostatic theory of the figure of the earth", Geophys. J., 8, 196-202, 1963.

Jordan, T. H. and W. S. Lynn, "A velocity anomaly in the lower mantle", J. Geophys. Res., 79, p. 2679-2685, 1974.

Julian, B. R. and M. K. Sengupta, "Seismic travel time evidence for lateral inhomogeneity in the deep mantle", Nature, 242, p. 443-447, 1973.

Kaula, W. M., "Elastic models of the mantle corresponding to variations in the external gravity field, *J. Geophys. Res.*, 68, 4967-4978, 1963.

Kaula, W. M., "Theory of Satellite Geodesy", Blaisdell Publishing Company, Waltham, Mass., 1966.

Kaula, W. M., "A tectonic classification of the main features of the earth's gravitational field", *J. Geophys. Res.*, 74, pp. 4807-4826, 1969.

Kaula, W. M., "Global gravity and tectonics", in *The Nature of the Solid Earth*, edited by E. C. Robertson, 385-405, McGraw-Hill, New York, 1972.

Kaula, W. M., "Geophysical inferences from statistical analyses of the gravity field", *Reports of the Department of Geodetic Sciences*, 250, Ohio State, Columbus, Ohio, pp. 119-141, 1977.

Khan, M. A., "Depth of sources of gravity anomalies", *Geophys. J. R. Astr. Soc.*, 48, 197-209, 1977.

Khan, M. A. and O'Keefe, J. A., "Relation of the Antarctic gravity low to the earth's equilibrium figure", 79, p. 3027-3030, 1974.

Khan, M. A. and G. P. Woollard, "Geophysical implications of the interrelationship of the geogravity and geomagnetic field", *Nature*, 226, 340-343, 1970.

King-Hele, D. G., D. M. C. Walker and R. H. Gooding, "Evaluations of harmonics in the geopotential of order 15 and odd degree", *Planet. Space Sci.*, 22, 1349-1373, 1974.

King-Hele, D. G., D. M. C. Walker and R. H. Gooding, "Geopotential harmonics of order 15 and even degree, from changes in orbital eccentricity at resonance", *Planet. Space Sci.* 1975, 23, 229-246, 1975.

Klolocnik, J., "Resonant coefficients of the earth's gravity field derived from the inclination of interkosmos satellites", *Bulletin of the Astronomical Institutes of Czechoslovakia* 26, 5, 293-300, 1975.

Lambeck, K., "Lateral density anomalies in the upper mantle", *J. Geophys. Res.*, 81, 6333-6339, 1976.

Lerch, F. J., Klosko, S. M., Laubscher, R. E., and Wagner, C. A., "Gravity model improvement using Geos-3 (GEM 9 & 10)", NASA/GSFC X-921-77-246, 1977.

MacDonald, G. J. F., "The deep structure of the continents", *Rev. Geophys.*, 1, 587-665, 1963.

MacMillan, W. D., "The Theory of the Potential", pp. 393, 405, Dover, New York, 1958.

McKenzie, D. P., J. M. Roberts, and N. O. Weiss, "Convection in the earth's mantle: Towards a numerical simulation", *J. Fluid Mech.*, 62, 465-538, 1974.

Marsh, B. D. and J. G. Marsh, "On global gravity anomalies and two-scale mantle convection", *J. Geophys. Res.*, 81, 5267-5280, 1976.

O'Connell, R. J., "Pleistocene glaciation and the viscosity of the lower mantle", *Geophys. J. R. Astr. Soc.*, 23, 299-327, 1971.

O'Connell, R. J., "On the scale of mantle convection", *Tectonophysics*, 38, 119-136, 1977.

Paul, M. K., "On computation of equal area blocks", *Bull. Geod.*, 107, 73-84, 1973.

Pollack, H. N., "Spherical harmonic representation of the gravitational potential of a point mass, a spherical cap, and a spherical rectangle", *J. Geophys. Res.*, 78, 1760-1768, 1973.

Press, F., "Earth models consistent with geophysical data", *Phys. Earth Planet. Int.*, 3, 3-22, 1970.

Rapp, R. H., "The relationship between mean anomaly block sizes and spherical harmonics", *J. Geophys. Res.*, 82, 5360-5364, 1977.

Richter, R. M., and B. Parsons, "One of the interaction of two scales of convection in the mantle", *J. Geophys. Res.*, 80, pp. 2529-2541, 1975.

Sclater, J. G., Lawver, L. A., and Parsons, B., "Comparison of long-wavelength residual elevation and free air gravity anomalies in the North Atlantic and possible implications for the thickness of the lithospheric plate", *J. Geophys. Res.*, 80, pp. 1031-1052, 1975.

Wagner, C. A., "The accuracy of Goddard earth models", NASA-GSFC X-921-76-187, 1976.

Wang, C., "Earth's zonal deformations", *J. Geophys. Res.*, 71, 1713-1720, 1966.